Altered Substrate Specificity in Flavocytochrome b_2: Structural Insights into the Mechanism of L-Lactate Dehydrogenation[†,‡]

Christopher G. Mowat,[§,||] Annemarie Wehenkel,[||] Amanda J. Green,[§] Malcolm D. Walkinshaw,[||] Graeme A. Reid,[||] and Stephen K. Chapman*[,§]

School of Chemistry, University of Edinburgh, West Mains Road, Edinburgh EH9 3JJ, United Kingdom, and Institute of Cell and Molecular Biology, University of Edinburgh, Mayfield Road, Edinburgh EH9 3JR, United Kingdom

Received April 14, 2004; Revised Manuscript Received May 14, 2004

ABSTRACT: Flavocytochrome b_2 from *Saccharomyces cerevisiae* is a L-lactate/cytochrome *c* oxidoreductase belonging to a large family of 2-hydroxyacid-dependent flavoenzymes. The crystal structure of the enzyme, with pyruvate bound at the active site, has been determined [Xia, Z.-X., and Mathews, F. S. (1990) *J. Mol. Biol. 212*, 837−863]. The authors indicate that the methyl group of pyruvate is in close contact with Ala198 and Leu230. These two residues are not well-conserved throughout the family of (*S*)-2-hydroxy acid oxidases/dehydrogenases. Thus, to probe substrate specificity in flavocytochrome b_2, these residues have been substituted by glycine and alanine, respectively. Kinetic studies on the L230A mutant enzyme and the A198G/L230A double mutant enzyme indicate a change in substrate selectivity for the enzyme toward larger (*S*)-2-hydroxy acids. In particular, the L230A enzyme is more efficient at utilizing (*S*)-2-hydroxyoctanoate by a factor of 40 as compared to the wild-type enzyme [Daff, S., Manson, F. D. C., Reid, G. A., and Chapman, S. K. (1994) *Biochem. J. 301*, 829−834], and the A198G/L230A double mutant enzyme is 6-fold more efficient with the aromatic substrate L-mandelate than it is with L-lactate [Sinclair, R., Reid, G. A., and Chapman, S. K. (1998) *Biochem. J. 333*, 117−120]. To complement these solution studies, we have solved the structure of the A198G/L230A enzyme in complex with pyruvate and as the FMN-sulfite adduct (both to 2.7 Å resolution). We have also obtained the structure of the L230A mutant enzyme in complex with phenylglyoxylate (the product of mandelate oxidation) to 3.0 Å resolution. These structures reveal the increased active-site volume available for binding larger substrates, while also confirming that the integrity of the interactions important for catalysis is maintained. In addition to this, the mode of binding of the bulky phenylglyoxylate at the active site is in accordance with the operation of a hydride transfer mechanism for substrate oxidation/flavin reduction in flavocytochrome b_2, whereas a mechanism involving the formation of a carbanion intermediate would appear to be sterically prohibited.

Flavocytochrome b_2 from *Saccharomyces cerevisiae* is a homotetrameric L-lactate dehydrogenase of subunit molecular weight 57.5 kDa. Each subunit consists of two distinct domains: a small (100 residue) N-terminal cytochrome domain containing protoheme IX and a large (411 residue) C-terminal domain containing flavin mononucleotide (FMN).[1] Substrate dehydrogenation occurs at the FMN, which is then reoxidized by stepwise transfer of electrons, via the b_2 heme, to cytochrome *c*. The structure of the native enzyme has been solved to 2.4 Å resolution (*1*) and reveals the existence of two crystallographically distinguishable subunits, one in which the heme domain is ordered (subunit A), and one in which the heme domain is disordered but pyruvate (the product of lactate dehydrogenation) is bound at the active site (subunit B). This visualization of pyruvate at the active site of the enzyme enabled the identification of residues important for substrate binding. Of these, Tyr143 and Arg376 are involved in binding the substrate carboxylate, while His373 and Tyr254 form hydrogen-bonding interactions with the α-keto oxygen of pyruvate. The pyruvate methyl group is in van der Waals contact with the side chains of Ala198 and Leu230.

Although L-lactate is the physiological substrate for Flavocytochrome b_2, the enzyme is also able to utilize other (*S*)-2-hydroxyacids. The substrate specificity of flavocytochrome b_2 has been strategically altered by site-directed mutagenesis to enable the enzyme to function more efficiently with long-chain 2-hydroxyacids (*2*). Construction of the A198G and L230A mutant enzymes, along with a double mutant incorporating both of these substitutions, resulted in a shifting of substrate selectivity toward larger 2-hydroxyacid substrates (*2*). In particular, the L230A mutant

[†] This work was supported by the U.K. Biotechnology and Biological Sciences Research Council (BBSRC) and by the Wellcome Trust funded Edinburgh Protein Interaction Centre (EPIC).

[‡] The atomic coordinates have been deposited in the Protein Data Bank [entries 1SZE (L230A with phenylglyoxylate bound), 1SZF (A198G/L230A with pyruvate bound), and 1SZG (A198G/L230A with sulfite bound)].

* Corresponding author. E-mail: S.K.Chapman@ed.ac.uk; fax/phone: (+44) 131 650 4760.

[§] School of Chemistry.

[||] Institute of Cell and Molecular Biology.

[1] Abbreviations: FMN, flavin mononucleotide; L230A, Leu230 → Ala mutation; A198G/L230A, Ala198 → Gly, Leu230 → Ala double mutation.

10.1021/bi049263m CCC: $27.50
Published on Web 06/30/2004

enzyme displayed increased selectivity (in terms of k_{cat}/K_m) for 2-hydroxyoctanoate over L-lactate by a factor of 40. Similarly, these mutant enzymes displayed an increased selectivity for the bulky aromatic substrate, L-mandelate, with the A198G/L230A double mutant enzyme having a 6-fold greater catalytic efficiency with L-mandelate than with L-lactate (*3*).

Flavocytochrome b_2 is a member of a large family of flavin-dependent oxidases and dehydrogenases that includes glycolate oxidase from spinach (*4*), D-amino acid oxidase (*5*), and L-mandelate dehydrogenases from *Rhodotorula graminis* (*6*) and *Pseudomonas putida* (*7*). It is believed that members of this family of enzymes all carry out substrate oxidation/flavin reduction via the same catalytic mechanism. However, there is conflicting evidence as to the nature of this process, and consequently, the precise mechanism of L-lactate oxidation in flavocytochrome b_2 has been a matter of much discussion, with two alternatives proposed. Both mechanisms have been reviewed previously (*8*, *9*). One of these includes the formation of a carbanion intermediate by the deprotonation of the lactate α-carbon by His373, the active site base (*10*). The other route involves the deprotonation of the lactate α-hydroxy group and transfer of the α-hydrogen to FMN as a hydride. The evidence for each of these possible mechanisms will be discussed in more detail later.

In an attempt to complement kinetic data obtained for the L230A and A198G/L230A mutant enzymes and to characterize the mode of substrate binding in these enzymes, we have obtained the crystal structure of the L230A enzyme in the presence of phenylglyoxylate (the product of mandelate oxidation) and the structures of the A198G/L230A enzyme in the presence of pyruvate and sulfite. In this paper, we describe these structures with reference to the altered substrate selectivity of these mutant enzymes and the relevance of the results to the mechanistic controversy.

MATERIALS AND METHODS

Both A198G/L230A and L230A mutant flavocytochromes b_2 were constructed, expressed, and produced as previously described by Daff et al. (*2*). Mutant enzymes were isolated according to the purification procedure reported elsewhere (*11*).

Crystallization and Refinement. Crystallization of both mutant flavocytochromes b_2 was carried out by hanging drop vapor diffusion in an air atmosphere at 20 °C in Linbro plates. In the case of the L230A mutant enzyme, crystals were obtained with a well solution comprising 100 mM sodium citrate buffer (pH 4.1−4.6), 200 mM NaBr, 12−15% PEG 3350, 18−20% glycerol, and 50 mM phenylglyoxylate. For the A198G/L230A protein in the presence of pyruvate, crystals were obtained with a well solution comprising 100 mM sodium citrate buffer (pH 4.1−4.6), 200 mM NaBr, 12−15% PEG 3350, 18−20% glycerol, and 50 mM pyruvate, and for the same mutant enzyme in the presence of sulfite, crystals were obtained with a well solution comprising 100 mM MES buffer (pH 5.5−6.5), 12−15% PEG 4000, 18−21% glycerol, and 50 mM sodium sulfite. In all cases, hanging drops (4 μL volume) were prepared by adding 2 μL of 15 mg/mL protein (in 10 mM TrisHCl pH 7.5, *I* 0.1) to 2 μL of well solution. After 1−3 days, large hexagonal crystals of up to 0.5 × 0.5 × 1 mm were formed. Because of the presence of glycerol in the mother liquor, crystals were mounted in nylon loops and flash-cooled in liquid nitrogen without the need for prior cryoprotectant soaking. For the L230A mutant enzyme in the presence of phenylglyoxylate, a data set was collected to 3.0 Å resolution at SRS Daresbury (station 14.2; $\lambda = 0.975$ Å). For the A198G/L230A enzyme in the presence of pyruvate, a data set was collected to 2.7 Å resolution at ESRF-Grenoble (beamline ID14-EH2; $\lambda = 0.934$ Å), and for the same mutant enzyme in the presence of sulfite, a data set was collected to 2.7 Å resolution at SRS Daresbury (station 9.6; $\lambda = 0.87$ Å). All data were collected using ADSC Quantum 4 detectors. In all cases, crystals were found to belong to space group $P3_221$. The L230A crystal was found to have cell dimensions $a = b = 163.027$ Å and $c = 112.473$ Å, the A198G/L230A with pyruvate had cell dimensions $a = b = 163.413$ Å and $c = 112.425$ Å, and the A198G/L230A with sulfite had cell dimensions $a = b = 163.966$ Å and $c = 112.508$ Å. Data processing was carried out using the HKL package (*12*). For the A198G/L230A enzyme in the presence of pyruvate and the L230A enzyme in the presence of phenylglyoxylate, the initial model for molecular replacement was the wild-type flavocytochrome b_2 structure (1FCB; ref *1*), stripped of water. In the case of the A198G/L230A enzyme in the presence of sulfite, the wild-type sulfite adduct structure (1LTD; ref *13*) was used as the molecular replacement model. Electron density fitting was carried out using the program TURBO-FRODO (*14*). Structure refinement was carried using Refmac5 (*15*). The atomic coordinates have been deposited in the Protein Data Bank, entries 1SZE (L230A with phenylglyoxylate), 1SZF (A198G/L230A with pyruvate), and 1SZG (A198G/L230A with sulfite).

RESULTS

In the case of the L230A mutant enzyme, a data set to 3.0 Å resolution was used to refine the structure to a final *R*-factor of 20.02% ($R_{free} = 24.92\%$) (Table 1). The final model consists of two protein molecules, subunit A and subunit B. Unlike the structure of the wild-type enzyme, in which one subunit has an ordered heme domain, the structure of the L230A mutant enzyme shows no interpretable density for the heme domain in either subunit, so these have been omitted from the model. Both subunits therefore consist of the flavodehydrogenase domain alone, each comprising residues Gly100 to Ala511, one FMN molecule, and one phenylglyoxylate molecule bound at the active site (Figure 1). In both subunits, there is a region of disordered polypeptide not observed in the density map, spanning residues Ser298 to Gly317 in subunit A and Ser298 to Arg320 in subunit B, as found in other structures of this and similar enzymes. The substitution of the Leu230 side chain by alanine is clearly observed in the electron density map. In addition, the model contains 124 water molecules. For the A198G/L230A mutant enzyme with pyruvate or sulfite bound, data sets to 2.7 Å resolution were used to refine the structures to final *R*-factors of 21.98% ($R_{free} = 25.33\%$) and 22.28% ($R_{free} = 26.57\%$), respectively (Table 1). As with the L230A mutant structure, both models consist of two flavodehydrogenase domains as described previously (except that in the sulfite-bound structure molecule B begins with

Table 1: Data Collection and Refinement Statistics

	L230A + phenylglyoxylate	A198G/L230A + pyruvate	A198G/L230A + sulfite
resolution (Å)	24.0−3.0	24.0−2.7	24.0−2.7
total no. of reflections	115354	497477	495303
no. of unique reflections	31503	47555	43777
completeness (%)	90.5	99.6	91.0
$I/[\sigma(I)]$	7.9	14.8	11.4
$I/[\sigma(I)]$ in outer shell (2.80−2.70 Å) (%) (3.11−3.00 Å*)	1.7*	4.8	2.7
R_{merge} (%)[a]	7.2	7.1	11.9
R_{merge} in outer shell (2.80−2.70 Å) (%) (3.11−3.00 Å*)	32.6*	20.2	60.3
R_{cryst} (%)[b]	20.02	21.98	22.28
R_{free} (%)[b]	24.92	25.33	26.57
rmsd from ideal values			
bond lengths (Å)	0.017	0.011	0.012
bond angles (deg)	1.9	1.6	1.6
Ramachandran analysis			
most favored (%)	84.3	89.4	88.9
additionally allowed (%)	15.3	9.9	10.5

[a] $R_{merge} = \Sigma_h\Sigma_i|I(h) - I_I(h)|/\Sigma_h\Sigma_i I_I(h)$, where $I_I(h)$ and $I(h)$ are the ith and mean measurement of reflection h, respectively. [b] $R_{cryst} = \Sigma_h|F_o - F_c|/\Sigma_h F_o$, where F_o and F_c are the observed and calculated structure factor amplitudes of reflection h, respectively. R_{free} is the test reflection data set, 5% selected randomly for cross validation during crystallographic refinement.

Thr102), with either pyruvate or sulfite bound (Figure 1). Sulfite is bound as an N5-sulfo-FMN adduct as found previously with structures of wild-type and R289K mutant flavocytochromes b_2 (*13*, *16*). In both models, the A198G/L230A substitutions are clearly seen in the electron density map. The disordered region of polypeptide in the model containing pyruvate comprises residues Thr300 to Gln316 in subunit A and Ser298 to Arg320 in subunit B. In the model containing sulfite, residues Lys301 to Arg320 in subunit A and Thr300 to Leu322 in subunit B are disordered and therefore absent from the model. In the case of the structure of the pyruvate-bound enzyme, there are 131 water molecules in the model and in the sulfite-bound enzyme, 170 waters. In all structures, both subunits are essentially identical, with rmsd fits for all backbone atoms of subunits A and B being 0.3 Å for the A198G/L230A enzyme with pyruvate bound and 0.4 Å for the other two structures. For all three structures, rmsd fits of all backbone atoms with the corresponding regions in the wild-type enzyme structures yield values of between 0.4 and 0.6 Å, indicating no significant global structural changes as a result of the substitutions.

In the structure of the L230A flavocytochrome b_2 with phenylglyoxylate bound at the active site, it can be clearly seen that the product molecule is bound in the same orientation as is observed for pyruvate in the wild-type enzyme (Figure 2), held at the carboxylate end by an electrostatic interaction with Arg376 and a hydrogen bond to Tyr143 (2.7 Å; distances quoted are the mean distances over both molecules A and B of the appropriate structure), and the α-keto oxygen forming hydrogen bonds with His373 (2.8 Å), the active site base, and Tyr254 (2.8 Å). The phenyl group of phenylglyoxylate is located adjacent to the Ala230 methyl group, oriented slightly away from the plane of the FMN isoalloxazine ring system, in a position that would be sterically prohibited in the wild-type enzyme due to the proximity of the Leu230 side chain (Figure 2). The α-carbon of the bound product is found to be 3.3 Å from N5 of FMN at an angle of approximately 113° from the plane of the isoalloxazine moiety, in the appropriate orientation for hydride transfer to N5 following deprotonation of the α-hydroxyl group by His373.

In the pyruvate-bound structure of the A198G/L230A double mutant enzyme, the product molecule is found to be in the same position as is seen in the structure of the wild-type enzyme (Figure 2), with the same electrostatic and hydrogen-bonding interactions as described previously for phenylglyoxylate. In this case, the α-carbon of pyruvate is found to be 3.7 Å from N5 of FMN at an angle of 122° from the plane of the flavin ring system. In the structure of the A198G/L230A enzyme with sulfite bound to N5 of FMN, sulfite interacts with active site residues in the same way as is observed in the structure of the wild-type enzyme (*13*), forming hydrogen bonds with His373 (3.1 Å), Arg376 (3.0 Å), Tyr143 (2.6 Å), and Tyr254 (2.7 Å) (Figure 2).

DISCUSSION

From the crystal structure of flavocytochrome b_2 with pyruvate bound at the active site, it can be seen that Ala198 and Leu230 are both in close contact with the pyruvate C2 methyl group (*1*). Consequently, it has been proposed that these residues are involved in conferring the enzyme's specificity for L-lactate. This idea is supported by the fact that in L-mandelate dehydrogenase, which utilizes a bulky aromatic substrate, the equivalent residues are glycine and alanine. In addition, glycolate oxidase, which operates on a substrate with hydrogen as the C2 substituent, has alanine and tryptophan as the residues equivalent to Ala198 and Leu230 in flavocytochrome b_2. An alignment of the amino acid sequence in the region around these residues in the three enzymes is shown in Figure 3. In this way, each enzyme has evolved with the optimal active site volume for its favored substrate. To investigate substrate specificity in flavocytochrome b_2, the L230A single and A198G/L230A double mutant forms of the enzyme were constructed and kinetically characterized with a range of (*S*)-2-hydroxy acids. The results of these studies have been reported previously by Daff et al. (*2*) and Sinclair et al. (*3*) and are summarized in Table 2. It can be seen from Table 2 that substitution of Leu230 enables more efficient utilization of larger substrates such as (*S*)-2-hydroxyoctanoate and L-mandelate. As a result, it was proposed that Leu230 is an important residue for L-lactate selectivity in flavocytochrome b_2, its substitution by alanine allowing more efficient binding of more sterically

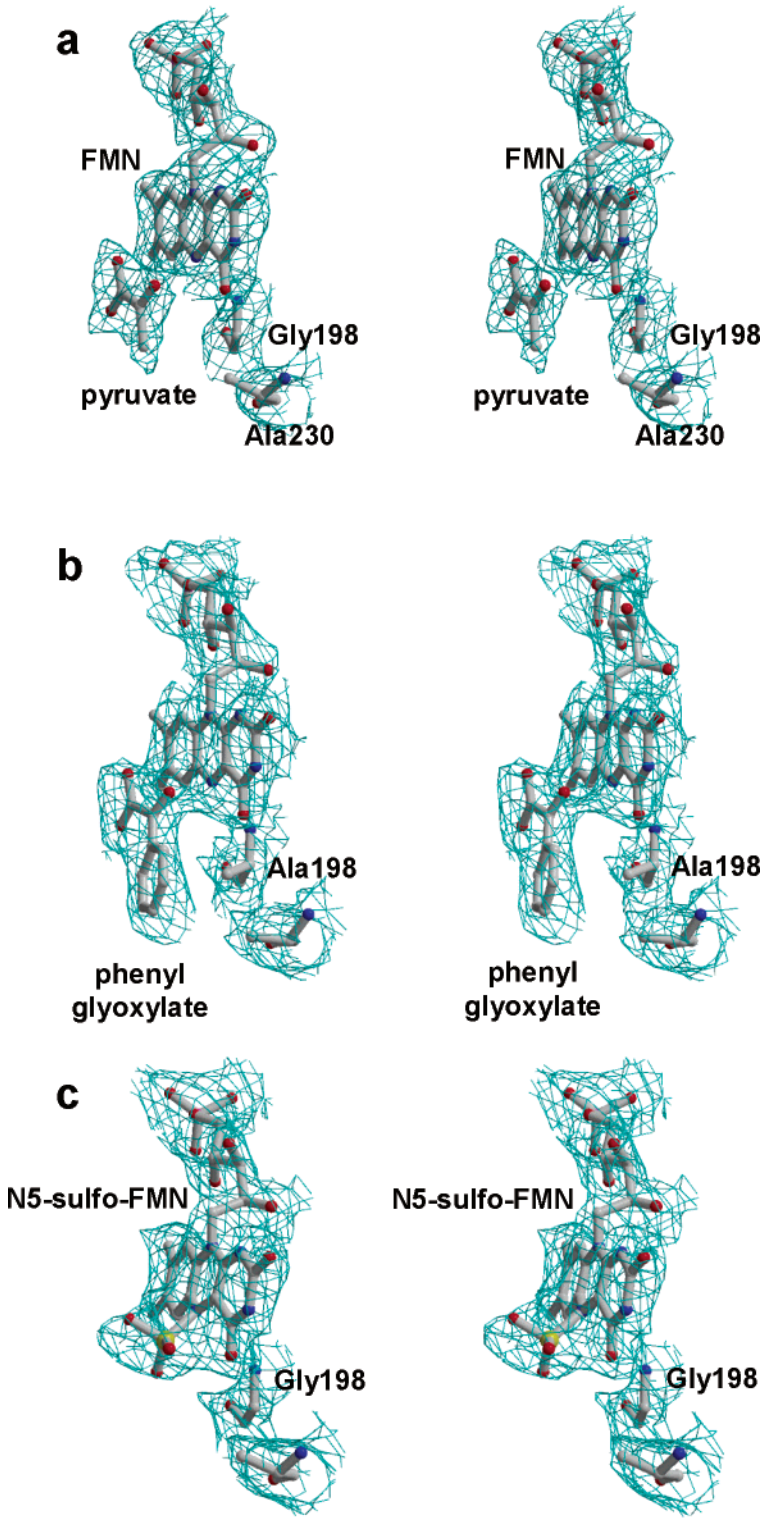

FIGURE 1: Stereoview of the electron density covering the FMN, the active site ligand, and the residues at position 198 and 230 in each structure. Panel a shows pyruvate bound at the active site of the A198G/L230A enzyme, panel b shows phenylglyoxylate bound at the active site of the L230A enzyme, and panel c shows the sulfite adduct of FMN in the A198G/L230A enzyme. The electron density maps were calculated using Fourier coefficients $2F_o - F_c$, where F_o and F_c are the observed and calculated structure factors, respectively, the latter based on the final model. The contour level is 1σ, where σ is the rms electron density. This figure was generated using BOBSCRIPT (*28*) and RASTER 3D (*29*).

bulky substrates. Indeed, the L230A mutant enzyme displays a 40-fold swing in selectivity (in terms of k_{cat}/K_m) for (*S*)-2-hydroxyoctanoate over L-lactate. The role of Ala198 is less clear, but the effect of its substitution by glycine is a general increase in K_M (relative to the L230A single mutant) for all substrates tested. The k_{cat} value of wild-type flavocytochrome b_2 with L-mandelate as substrate is very low but is increased 5-fold by the introduction of the L230A mutation, while additional substitution of Ala198 by glycine results in a double mutant enzyme with a k_{cat} for mandelate that is 400-fold greater than the wild-type enzyme. In fact, the A198G/L230A enzyme is 6-fold more efficient with L-mandelate as

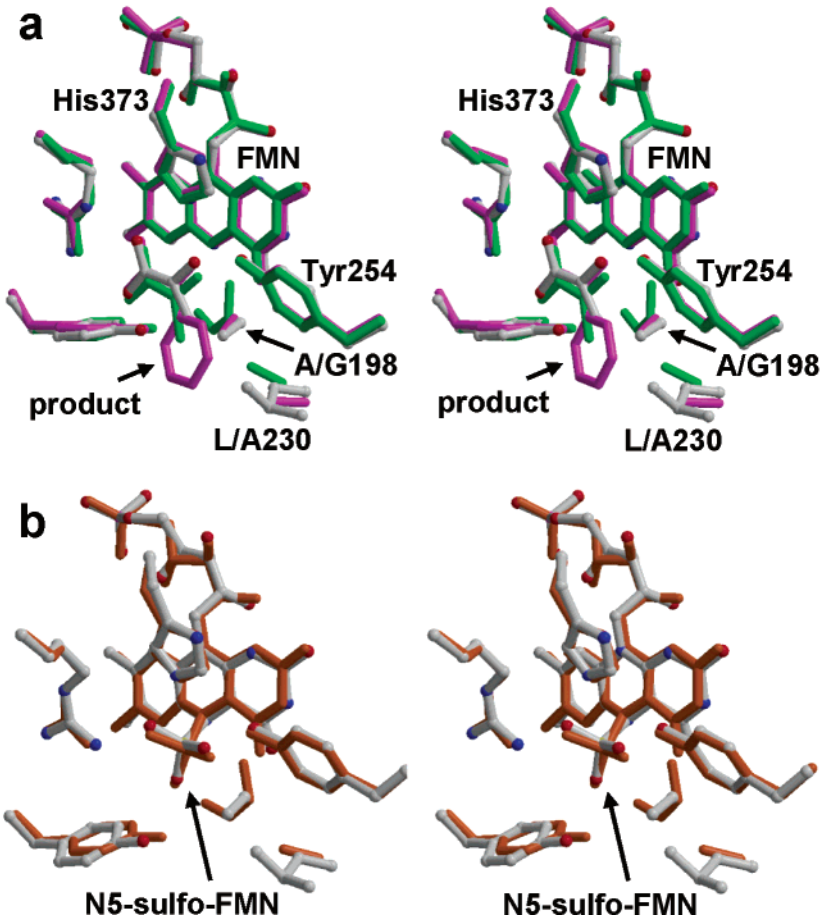

FIGURE 2: (a) Stereoview of the overlaid active sites of wild-type flavocytochrome b_2 with pyruvate bound (atom type color), A198G/L230A enzyme with pyruvate bound (green), and L230A enzyme with phenylglyoxylate bound (magenta). (b) Stereoview of the overlaid active sites of wild-type flavocytochrome b_2 with sulfite bound to FMN (atom type color) and A198G/L230A enzyme with sulfite bound (orange). This figure was generated using BOBSCRIPT (*28*) and RASTER 3D (*29*).

```
                                                198
                                                 ↓
S. cerevisiae b2    LVDVRKVDIS TDMLGSHVDV PFYVSATALC KLGNPLEGEK DVARGCGQGV 220
Spinach GOx         LIDVTNIDMT TTILGFKISM PIMIAPTAMQ KMAHP-EGEY ATARAASAA- 95
P. putida L-MDH     LVDVSRRSLQ AEVLGKRQSM PLLIGPTGLN GALWP-KGDL ALARAATKA- 97

                          230
                           ↓
S. cerevisiae b2    TKVPQMISTL ASCSPEEIIE AAPSDKQIQW YQLYVNSDRK ITDDLVKNVE 270
Spinach GOx         -GTIMTLSSW ATSSVEEVAS TGP-G--IRF FQLYVYKDRN VVAQLVRRAE 145
P. putida L-MDH     -GIPFVLSTA SNMSIEDLAR QC-DGD--LW FQLYVIH-RE IAQGMVLKAL 146
```

FIGURE 3: Alignment of the amino acid sequences of flavocytochrome b_2, spinach glycolate oxidase, and *Pseudomonas putida* L-mandelate dehydrogenase for the region surrounding Ala198 and Leu230 of flavocytochrome b_2. Ala198 and Leu230 are shown in red, along with their equivalents in the other sequences.

substrate than with L-lactate (as indicated by k_{cat}/K_M values).

To further probe the role of these two residues in substrate binding and catalysis, we have crystallized the A198G/L230A double mutant enzyme in the presence of pyruvate (the product of L-lactate oxidation) and sulfite (an inhibitor of the enzyme that is known to form a reversible adduct with FMN (*12*)) and the L230A enzyme in the presence of phenylglyoxylate (the product of L-mandelate oxidation). It is apparent from all of these structures that removal of the steric bulk of the Leu230 side chain creates an increased volume to accommodate the binding of larger substrates at the active site of flavocytochrome b_2, as can be seen in Figure 2. What is also apparent from Figure 2 is that there are no other changes in the active site, with the positions of the important catalytic residues being preserved in the mutant enzyme structures. It can be seen from Table 2 that for longer chain aliphatic substrates such as (*S*)-2-hydroxyoctanoate, the effect of the substitutions of Leu230 and Ala198 is more of a shift in activity away from L-lactate rather than toward longer chain substrates. However, in the case of the aromatic substrate L-mandelate, wild-type flavocytochrome b_2 has barely detectable dehydrogenase activity, and this is increased to very significant levels by the substitution(s). It is interesting to note that in the homologous L-mandelate dehydrogenases from *Rhodotorula graminis* (which is also a flavocytochrome b_2 (*6*)) and *Pseudomonas putida* (*7*), the residues equivalent to Ala198 and Leu230 in L-lactate dehydrogenase are both glycine. This is in line with the larger active site volume necessary for mandelate binding and turnover, but as yet no structure of a mandelate dehydrogenase is available

Table 2: Kinetic Parameters for Wild-Type, L230A, and A198G/L230A Flavocytochromes b_2 with L-Lactate, L-Mandelate, and (*S*)-2-Hydroxyoctanoate as Substrates[a]

enzyme	parameter	substrate		
		L-lactate[b]	L-mandelate[c]	(*S*)-2-hydroxyoctanoate[b]
wild-type	k_{cat} (s^{-1})	400 ± 10	0.02 ± 0.01[d]	45 ± 5
	K_M (mM)	0.49 ± 0.05	nd[d,e]	0.11 ± 0.01
	k_{cat}/K_M (mM^{-1} s^{-1})	816 ± 116	nd[d,e]	410 ± 60
L230A	k_{cat} (s^{-1})	30 ± 3	0.11 ± 0.05	52 ± 5
	K_M (mM)	6.1 ± 0.2	0.16 ± 0.01	0.23 ± 0.01
	k_{cat}/K_M (mM^{-1} s^{-1})	4.9 ± 0.7	0.69 ± 0.38	226 ± 24
A198G/L230A	k_{cat} (s^{-1})	41 ± 2	8.50 ± 0.50	68 ± 3
	K_M (mM)	38 ± 4	1.36 ± 0.10	1.9 ± 0.1
	k_{cat}/K_M (mM^{-1} s^{-1})	1.08 ± 0.15	6.25 ± 0.89	36 ± 3

[a] In all cases, experiments were carried out at 25 ± 0.1 °C in 10 mM TrisHCl buffer at pH 7.5 (I = 0.10), with ferricyanide (1 mM) as electron acceptor. Values of k_{cat} are expressed as electrons transferred per second per molecule of enzyme. All errors quoted represent standard deviations from a nonlinear least-squares fit. [b] All values taken from ref *2*. [c] All values taken from ref *3*. [d] In another study (*26*) under different experimental conditions (30 °C, 0.1 M Na^+/K^+ phosphate buffer, 1 mM EDTA, pH 7.0), k_{cat} was found to be 0.012 ± 0.002 s^{-1}, K_M to be 0.380 ± 0.060 mM, and k_{cat}/K_M to be 0.031 ± 0.003 mM^{-1} s^{-1}. [e] nd = not determined. In the case of the wild-type enzyme with L-mandelate as substrate, activities were so low that it was impossible to determine a meaningful K_M value.

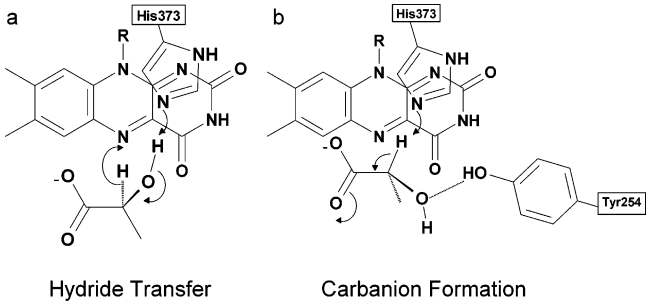

FIGURE 4: Mechanisms for lactate dehydrogenation. (a) By hydride transfer: His373 abstracts the hydroxyl proton and promotes hydride transfer to the N5 of FMN. (b) By carbanion formation: His373 removes the α-carbon hydrogen as a proton forming a carbanion. A subsequent transfer of two electrons to the flavin is required.

with mandelate or phenylglyoxylate at the active site.

The precise mechanism of substrate oxidation in the family of 2-hydroxy acid dehydrogenases and oxidases has been the subject of much controversy, with two alternate mechanisms proposed. These are illustrated in Figure 4. The operation of a mechanism involving a carbanion intermediate involves deprotonation of the substrate α-carbon by a catalytic base (His373 in flavocytochrome b_2) (*10*) and subsequent transfer of reducing equivalents to the flavin to yield reduced FMN and pyruvate (*9*). Much of the fundamental work that led to the proposal of a carbanion mechanism for this flavoenzyme superfamily was carried out on the related enzyme D-amino acid oxidase (*17*, *18*). Intriguingly, the high-resolution structure of D-amino acid oxidase (*19*) reveals that there is no active site base catalyst in the enzyme and that in complex with D-trifluoroalanine, the α-C−H of the ligand is oriented toward FAD N5, leading to the conclusion that oxidation of the substrate must occur via a hydride transfer mechanism. In addition, crystallographic studies have been carried out on D-amino acid oxidase with the bulky reaction product iminotryptophan bound at the active site (*20*). Assuming a similar mode of binding for the substrate, D-tryptophan, steric constraints would result in orientation of the substrate α-H toward FAD in a manner consistent with the operation of a hydride transfer mechanism.

The hydride transfer mechanism requires deprotonation of the substrate α-hydroxyl group (by His373 in flavocytochrome b_2) and transfer of the α-hydrogen to FMN N5 as a hydride (*16*). There are many publications that present evidence for the operation of each of the proposed mechanisms. Central to the operation of a carbanion mechanism is the notion that Tyr254, an active site residue, forms a hydrogen bond with the α-hydroxyl group of L-lactate in the Michaelis complex. In this way, it is proposed to orient the substrate α-hydrogen toward His373 for deprotonation to occur or, if Tyr254 were itself deprotonated, to act as a second base facilitating flavin reduction by removing a second proton from the α-hydroxyl group of the carbanion intermediate. However, studies on Tyr254-substituted forms of the enzyme where the residue at this position now has no ability to form such a hydrogen bond in the Michaelis complex indicate that although enzyme activity is impaired as a consequence of such substitutions, there is no increase in L-lactate K_M values, thus ruling out such a role in substrate binding (*21*). In fact, the effects of the Y254 substitutions on k_{cat} indicate that this residue is involved in transition state stabilization. Recent primary and solvent kinetic isotope studies on both the wild-type and the Y254F mutant enzymes conclude that a concerted cleavage of both α-CH and α-OH occurs in the Y254F mutant enzyme, consistent with a hydride transfer mechanism, while stepwise cleavage of these two bonds in the wild-type enzyme is explained by the existence of a deprotonated lactate alkoxide intermediate that collapses upon transfer of the α-H to FMN as a hydride (*22*, *23*).

Recent work in support of a carbanion mechanism has been carried out on the (*S*)-mandelate dehydrogenase from *Pseudomonas putida* (*24*, *25*). Using L-mandelate and both ethyl and methyl esters of L-mandelic acid as substrates, these workers were able to detect a transient intermediate formed during FMN reduction. This intermediate is characteristic of a charge-transfer complex between oxidized FMN and an electron-rich donor and is suggested to be a carbanion/enolate intermediate generated by base-catalyzed abstraction of the substrate α-proton. However, such a finding is also in line with the existence of an electron-rich deprotonated alkoxide intermediate, formed from L-lactate by α-hydroxyl deprotonation, as proposed by Sobrado et al. (*23*) for flavocytochrome b_2.

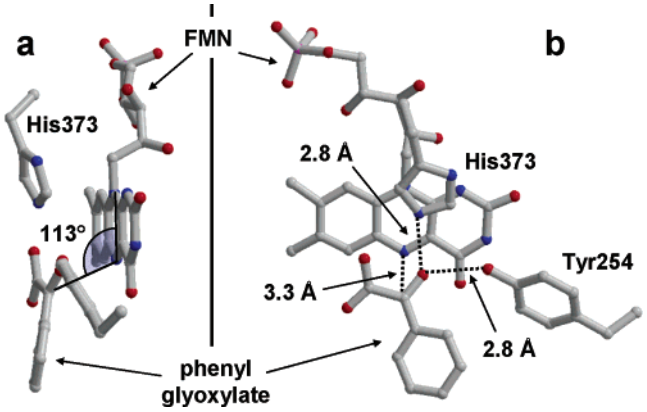

FIGURE 5: Interaction of phenylglyoxylate at the active site of L230A flavocytochrome b_2. Panel a shows a side view, revealing the angle between the α-carbon and the plane of the flavin to be 113°. Panel b, the front view, shows the hydride transfer distance of 3.3 Å and the interaction of the α-carbonyl oxygen with His373 and Tyr254. This figure was generated using BOBSCRIPT (*28*) and RASTER 3D (*29*).

The stereochemistry of L-lactate dictates that for either mechanism a different mode of binding is necessary. For removal of the a-proton by His373, it is clear that the angle between the C2−C3 bond and the plane of the carboxylate group must differ from the orientation required for deprotonation of the α-hydroxyl group. The presence of the sp^2 hybridized product molecule leaves the arrangement of the Michaelis complex open to question. However, in the case of the mutant enzymes described in this paper, which have altered substrate selectivity and relatively high affinity for bulkier substrates such as L-mandelate, it is unlikely that two modes of substrate binding would be possible due to steric constraints. Modeling studies have been carried out using the pyruvate-bound wild-type structure of flavocytochrome b_2 (*26*). With L-lactate modeled at the active site in the appropriate orientation for either carbanion or hydride transfer mechanism, there is little to suggest that either orientation would be preferred on structural grounds. However, when positioned optimally for α-proton abstraction by His373, the substrate α-hydroxyl group is shown to form a hydrogen bond with the phenolic side chain of Tyr254, an interaction that appears unlikely to occur based upon solution studies of Tyr254-substituted enzymes (*21*). Modeling of L-mandelate at the active site of wild-type flavocytochrome b_2 indicates that in this case the presence of the bulky phenyl group of the substrate would prevent substrate binding in the appropriate orientation for α-proton abstraction by His373, and it is suggested that in this case at least, hydride transfer must occur (*26*). This conclusion is now corroborated by our structure of the phenylglyoxylate-bound L230A flavocytochrome b_2 presented in this work. As can be seen from Figures 2a and 5, phenylglyoxylate binds in the same orientation as pyruvate found in the active site of the wild-type enzyme, forming hydrogen bonds between the α-keto group and His373 and Tyr254. The phenyl group is oriented slightly away from the plane of the FMN ring system, in a position that would be sterically prohibited in the wild-type enzyme due to the presence of the Leu230 side chain. Figure 6 shows L-mandelate modeled at the active site of L230A flavocytochrome b_2 in an orientation suitable for α-H removal by His373 and carbanion formation. From this figure, it can be seen that this would result in the phenyl ring of the substrate being impossibly close to the FMN and the side chains of Ala198 and Ser228 at distances of 1.7, 1.1, and 2.2 Å, respectively.

The position of the phenylglyoxylate α-carbon is also mechanistically significant. Fraaije and Mattevi (*27*) have carried out a comparison of the structures of several flavoenzymes in complex with product molecules or substrate analogues. One of the findings of this work is that in each case the ligand atom that mimics the substrate atom dehydrogenated by the flavin is found in a very similar position. In this way, the site of oxidative attack by the flavin is typically found to be 3.5 Å from the flavin N5, at an angle of 96−117° from the N5−N10 axis. In the case of phenylglyoxylate bound to flavocytochrome b_2, the α-carbon is found to be 3.3 Å from N5 of FMN at an angle of 113° from the FMN N5−N10 axis. This is in accordance with the values quoted by Fraaije and Mattevi, placing the α-carbon in a position appropriate for hydride transfer to

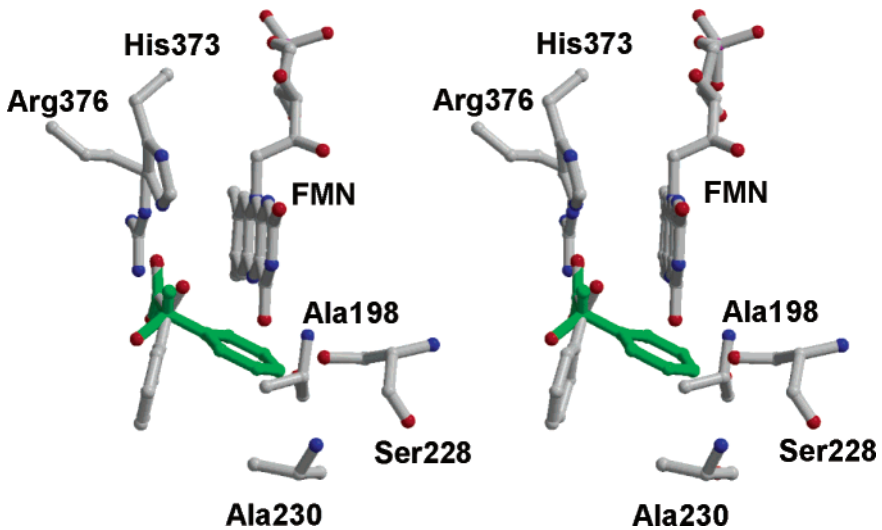

FIGURE 6: Stereoview of L-mandelate (green) modeled at the active site of L230A flavocytochrome b_2 in the orientation that would be required for carbanion formation. Phenylglyoxylate is shown in atom type colors. This positioning of the phenyl ring of L-mandelate places it 1.7 Å from FMN, 1.1 Å from the side chain of Ala198, and 2.2 Å from Ser228 and is therefore clearly sterically prohibited. This figure was generated using BOBSCRIPT (*28*) and RASTER 3D (*29*).

FMN N5 following deprotonation of the α-hydroxyl by His373. Although phenylglyoxylate is the product of mandelate oxidation, it is obvious that in this mutant enzyme, which is an active L-mandelate dehydrogenase, the formation of a carbanion intermediate would require a substantially different mode of binding of L-mandelate. This would result in the substrate phenyl ring pointing toward the flavin, which is clearly sterically impossible.

ACKNOWLEDGMENT

We thank SRS Daresbury and ESRF Grenoble for access to synchrotron facilities.

REFERENCES

1. Xia, Z.-x., and Mathews, F. S. (1990) Molecular structure of flavocytochrome b_2 at 2.4 Å resolution, *J. Mol. Biol. 212*, 837−863.
2. Daff, S., Manson, F. D. C., Reid, G. A., and Chapman, S. K. (1994) Strategic manipulation of the substrate specificity of *Saccharomyces cerevisiae* flavocytochrome b_2, *Biochem. J. 301*, 829−834.
3. Sinclair, R., Reid, G. A., and Chapman, S. K. (1998) Redesign of Saccharomyces cerevisiae flavocytochrome b_2: Introduction of L-mandelate dehydrogenase activity, *Biochem. J. 333*, 117−120.
4. Lindqvist, Y., Bränden, C.-I., Mathews, F. S., and Lederer, F. (1991) Spinach glycolate oxidase and yeast flavocytochrome b_2 are structurally homologous and evolutionarily related enzymes with distinctly different function and FMN binding, *J. Biol. Chem. 266*, 3198−3207.
5. Mattevi, A., Vanoni, M. A., Todone, F., Rizzi, M., Teplyakov, A., Coda, A., Bolognesi, M., and Curti, B. (1996) Crystal structure of D-amino acid oxidase: a case of active site mirror-image convergent evolution with flavocytochrome b_2, *Proc. Natl. Acad. Sci. U.S.A. 93*, 7496−7501.
6. Ilias, R. M., Sinclair, R., Robertson, D., Neu, A., Chapman, S. K., and Reid, G. A. (1998), L-Mandelate dehydrogenase from *Rhodotorula graminis*, *Biochem. J. 333*, 107−115.
7. Tsou, A. Y., Ransom, S. C., Gerlt, J. A., Buechter, D. D., Babbitt, P. C., and Kenyon, G. L. (1990) Mandelate pathway of *Pseudomonas putida*: Sequence relationships involving mandelate racemase, (*S*)-mandelate dehydrogenase, and benzoylformate decarboxylase and expression of benzoylformate decarboxylase in *Escherichia coli*, *Biochemistry 29*, 9856−9862.
8. Mowat, C. G., and Chapman, S. K. (2000) Flavocytochrome b_2, in *Subcellular Biochemistry, Volume 35: Enzyme-Catalyzed Electron and Radical Transfer* (Holzenburg, A., Scrutton, N. S., Eds.) pp 279−295, Kluwer Academic/Plenum Publishers, New York.
9. Ghisla, S., and Massey, V. (1989) Mechanisms of flavoprotein-catalyzed reactions, *Eur. J. Biochem. 181*, 1−17.
10. Lederer, F. (1991) Flavocytochrome b_2, in *Chemistry and Biochemistry of Flavoenzymes Volume 2* (Muller, F., Ed.) pp 153−242, CRC Press, Boca Raton, FL.
11. Black, M. T., White, S. A., Reid, G. A., and Chapman, S. K. (1989) High-level expression of fully active yeast flavocytochrome b_2 in *Escherichia coli*, *Biochem. J. 258*, 255−259.
12. Otwinowski, Z., and Minor, W. (1997) Processing of X-ray diffraction data collected in oscillation mode, *Methods Enzymol. 276*, 307−326.
13. Tegoni, M., and Cambillau, C. (1994) The 2.6 Å refined structure of the *Escherichia coli* recombinant *Saccharomyces cerevisiae* flavocytochrome b_2 sulfite complex, *Protein Sci. 3*, 303−313.
14. Roussel, A., and Cambillau, C. (1991) TURBO−FRODO, in *Silicon Graphics Geometry Partners Directory 86*, Silicon Graphics, Mountain View, CA.
15. Murshudov, G. N., Vagin, A. A., and Dodson, E. J. (1997) Refinement of macromolecular structures by the maximum-likelihood method, *Acta Crystallogr. D53*, 240−255.
16. Mowat, C. G., Beaudoin, I., Durley, R. C., Barton, J. D., Pike, A. D., Chen, Z. W., Reid, G. A., Chapman, F. S., Mathews, F. S., and Lederer, F. (2000) Kinetic and crystallographic studies on the active site Arg289Lys mutant of flavocytochrome b_2 (yeast L-lactate dehydrogenase), *Biochemistry 39*, 3266−3275.
17. Walsh, C. T., Schonbrunn, A., Lockridge, O., Massey, V., and Abeles, R. (1972) Inactivation of a flavoprotein, lactate oxidase, by an acetylenic substrate, *J. Biol. Chem. 247*, 6004−6006.
18. Walsh, C. T., Lockridge, O., Massey, V., and Abeles, R. (1973) Studies on the mechanism of action of the flavoenzyme lactate oxidase. Oxidation and elimination with β-chlorolactate, *J. Biol. Chem. 248*, 7049−7054.
19. Umhau, S., Pollegioni, L., Molla, G., Diederichs, K., Welte, W., Pilone, M. S., and Ghisla, S. (2000) The X-ray structure of D-amino acid oxidase at very high resolution identifies the chemical mechanism of flavin-dependent substrate dehydrogenation, *Proc. Natl. Acad. Sci. U.S.A. 97*, 12463−12468.
20. Todone, F., Vanoni, M. A., Mozzarelli, A., Bolognesi, M., Coda, A., Curti, B., and Mattevi, A. (1997) Active site plasticity in D-amino acid oxidase: A crystallographic analysis, *Biochemistry 36*, 5853−5860.
21. Dubois, J., Chapman, S. K., Mathews, F. S., Reid, G. A., and Lederer, F. (1990) Substitution of Tyr254 with Phe at the active site of flavocytochrome b_2, *Biochemistry 29*, 6393−6400.
22. Sobrado, P., Daubner, S. C., and Fitzpatrick, P. F. (2001) Probing the relative timing of hydrogen abstraction steps in the flavocytochrome b_2 reaction with primary and solvent deuterium isotope effects and mutant enzymes, *Biochemistry 40*, 994−1001.
23. Sobrado, P., and Fitzpatrick, P. F. (2003) Solvent and primary deuterium isotope effects show that lactate CH and OH bond cleavages are concerted in Y254F flavocytochrome b_2, consistent with a hydride transfer mechanism, *Biochemistry 42*, 15208−15214.
24. Dewanti, A. R., and Mitra, B. (2003) Transient intermediate in the reaction catalyzed by (*S*)-mandelate dehydrogenase from *Pseudomonas putida*, *Biochemistry 42*, 12893−12901.
25. Dewanti, A. R., Xu, Y., and Mitra, B. (2004) Esters of mandelic acid as substrates for (*S*)-mandelate dehydrogenase from *Pseudomonas putida*: Implications for the reaction mechanism, *Biochemistry 43*, 1883−1890.
26. Gondry, M., Dubois, J., Terrier, M., and Lederer, F. (2001) The catalytic role of tyrosine 254 in flavocytochrome b_2 (L-lactate dehydrogenase from baker's yeast), *Eur. J. Biochem. 268*, 4918−4927.
27. Fraaije, M. W., and Mattevi, A. (2000) Flavoenzymes: diverse catalysts with recurrent features, *Trends Biochem. Sci. 5*, 126−132.
28. Esnouf, R. M. (1997) An extensively modified version of MolScript that includes greatly enhanced coloring capabilities, *J. Mol. Graph. 15*, 132−134.
29. Merritt, E. A., and Murphy, M. E. P. (1994) *Raster*3D version 2.0: A program for photorealistic molecular graphics, *Acta Crystallogr. D50*, 869−873.

BI049263M